The Astrophysical Journal, 927:55 (9pp), 2022 March 1 https://doi.org/10.3847/1538-4357/ac4c42

On the Fast Radio Burst and Persistent Radio Source Populations

Casey J. Law[1,2], Liam Connor[1], and Kshitij Aggarwal[3,4]
[1] Cahill Center for Astronomy and Astrophysics, MC 249-17 California Institute of Technology, Pasadena, CA 91125, USA
[2] Owens Valley Radio Observatory, California Institute of Technology, 100 Leighton Lane, Big Pine, CA 93513, USA
[3] West Virginia University, Department of Physics and Astronomy, P.O. Box 6315, Morgantown, WV 26506-6315, USA
[4] Center for Gravitational Waves and Cosmology, West Virginia University, Chestnut Ridge Research Building, Morgantown, WV 26506-6315, USA
Received 2021 October 22; revised 2022 January 14; accepted 2022 January 16; published 2022 March 4

Abstract

The first fast radio burst (FRB) to be precisely localized was associated with a luminous persistent radio source (PRS). Recently, a second FRB/PRS association was discovered for another repeating source of FRBs. However, it is not clear what makes FRBs or PRS or how they are related. We compile FRB and PRS properties to consider the population of FRB/PRS sources. We suggest a practical definition for PRS as FRB associations with luminosity greater than 10^{29} erg s^{-1} Hz^{-1} that are not attributed to star formation activity in the host galaxy. We model the probability distribution of the fraction of FRBs with PRS for repeaters and nonrepeaters, showing there is not yet evidence for repeaters to be preferentially associated with PRS. We discuss how FRB/PRS sources may be distinguished by the combination of active repetition and an excess dispersion measure local to the FRB environment. We use CHIME/FRB event statistics to bound the mean per-source repetition rate of FRBs to be between 25 and 440 yr^{-1}. We use this to provide a bound on the density of FRB-emitting sources in the local universe of between 2.2×10^2 and 5.2×10^4 Gpc^{-3} assuming a pulsar-like beamwidth for FRB emission. This density implies that PRS may comprise as much as 1% of compact, luminous radio sources detected in the local universe. The cosmic density and phenomenology of PRS are similar to that of the newly discovered, off-nuclear "wandering" active galactic nuclei (AGN). We argue that it is likely that some PRS have already been detected and misidentified as AGN.

Unified Astronomy Thesaurus concepts: Magnetars (992); Radio bursts (1339); Radio source counts (1357)

1. Introduction

Several hundred fast radio burst (FRB) sources have been identified in the last decade (Lorimer et al. 2007; Cordes & Chatterjee 2019; Petroff et al. 2019; The CHIME/FRB Collaboration et al. 2021). Recent observational efforts have focused on localizing FRBs to arcsecond precision in order to associate the burst to multiwavelength counterparts (Macquart et al. 2010; Law et al. 2018a; Kocz et al. 2019; Heintz et al. 2020; Marcote et al. 2020; Oostrum et al. 2020; Bhandari et al. 2022; Rajwade et al. 2021). Roughly two dozen FRBs have been localized to this precision and associated with a host galaxy with a spectroscopic distance. This sample of FRBs has been used to characterize the stellar environment of FRBs (Mannings et al. 2021; Tendulkar et al. 2021), study the FRB local magneto-ionic environment (Michilli et al. 2018; Hilmarsson et al. 2021), and measure the baryon density of the intergalactic medium (Macquart et al. 2020).

Roughly 25 FRB sources are known to emit multiple bursts (e.g., CHIME/FRB Collaboration et al. 2019), a few of which may exhibit periodic modulation to their burst rate (Chime/Frb Collaboration et al. 2020; Rajwade et al. 2020). The discovery of repeating FRBs has had a large impact on the question of FRB origin, both because they demonstrate that some bursts are not cataclysmic and because repetition makes the sources easier to localize. Eight repeating FRBs have so far been localized precisely enough to be associated with a host galaxy (Heintz et al. 2020; Marcote et al. 2020; Law et al. 2021).

The first repeating FRB, known as 121102, was both the first to be localized and the first to be associated with a luminous persistent radio source (PRS; Chatterjee et al. 2017). The PRS has a luminosity of $L_{1.4\,\mathrm{GHz}} = 2 \times 10^{29}$ erg s^{-1} Hz^{-1}, comparable to a low-luminosity active galactic nucleus (AGN). The emission is isotropic, incoherent synchrotron radiation, which has been theoretically modeled to probe the FRB environment (Murase et al. 2016; Margalit & Metzger 2018; Katz 2021). In this way, FRB 121102 motivated new, more detailed models for FRB origins through constraints on the characteristic age and energy density of the FRB environment. However, it remained the only example FRB/PRS association after the next dozen FRBs were localized, so its relevance to the overall FRB population was unclear.

The recent discovery of FRB 20190520 (hereafter 190520) has changed this view dramatically. The source is similar to FRB 121102 in its burst activity, host galaxy properties, and association with a PRS (Niu et al. 2021). We now know that PRS are an important part of the lives of some FRBs, but it is not clear how common they are. Given that FRBs occur with a high volumetric rate (comparable to that of core-collapse supernovae; Luo et al. 2018; Perley et al. 2020) and that PRS are luminous, it may be that PRS constitute a significant new class of extragalactic radio source.

A related open question is whether all FRBs are emitted by a single kind of source or if there are multiple sources of FRBs.[5] While it is currently not known if the origin of repeating FRBs and (apparent) nonrepeaters are physically distinct, there is

[5] We use the word "source" to refer to a physical object formed in a particular way. By considering the formation channel in the definition of a source, one can distinguish between, say, a magnetar formed via a core-collapse supernova and one formed via accretion-induced collapse.

emerging evidence for differences in their burst properties. Repeating FRBs tend to be wider in duration and narrower in bandwidth than once-off events (CHIME/FRB Collaboration et al. 2019; Fonseca et al. 2020; Pleunis et al. 2021). However, Connor et al. (2020a) noted that viewing angle selection effects may explain effects like those observed. If PRS properties are causally connected to FRB properties, then it offers new ways to test the multiple-origin hypothesis.

Here, we consider the occurrence of PRS in FRBs, their prevalence in the local universe, and correlations between FRB and PRS properties. The goal of this analysis is to consider the FRB/PRS as a new class of radio source and discuss how to use them to test models of FRB origin. Section 2 compiles measurements of the FRB/PRS population and suggests physically motivated definitions of subpopulations of FRBs. Section 3 uses these definitions to demonstrate a preference for repeating FRBs to be associated with PRS. In Section 4, we discuss correlations between observed FRB and PRS properties. Section 5 discusses the volumetric density of the FRB population, and Section 6 discusses how PRS can be identified independently of FRBs.

2. FRB and PRS Populations

To begin, we compile measurements of FRB and PRS sources. Since the detection of an FRB or PRS is sensitive to the quality of data, it is important to have physically motivated definitions for the "FRB," "PRS," and "repeating" classes. PRS are most easily identified for localized FRBs, so we focus on that subset of all FRB sources.

For the first ten years of study of FRBs, the practical definition of the source was a millisecond radio transient that was highly dispersed.[6] For FRBs with DMs in excess of that expected from the Milky Way, their implied distances—and luminosities—were many orders of magnitude larger than those of Galactic millisecond transients like pulsars.

The discovery of a luminous radio burst from a magnetar in the Milky Way (SGR 1935+2154; Bochenek et al. 2020; CHIME/FRB Collaboration et al. 2020) made it clear that FRBs require an explicit luminosity definition. It has also become simpler to define the FRB class by its luminosity as more FRBs are associated with host galaxies. Therefore, we propose an FRB radio spectral energy threshold of 10^{29} erg Hz^{-1}, which includes all FRBs and excludes all other millisecond radio transients associated with well-defined Galactic classes (e.g., Crab giant pulses; Cordes et al. 2004; Lyu et al. 2021). With this definition, a repeating FRB is defined as any source with multiple bursts with energy greater than 10^{29} erg Hz^{-1}.

A practical definition of a PRS should include the two well-characterized sources and exclude other classes of radio source. We suggest defining a PRS as an FRB associated radio source with a spectral luminosity[7] $L_\nu > 10^{29}$ erg s^{-1} Hz^{-1} that is not attributed to star formation activity in the host galaxy. Individual supernova remnants and star formation regions observed are far less luminous than this threshold (Parra et al. 2007). Radio emission related to active star formation throughout the galaxy can be excluded through VLBI measurements or constraints on the star formation rate (Fong et al. 2021; Ravi et al. 2021). The PRS luminosity limit also excludes all known typed supernovae (relativistic explosions such as SN Ic-BL are also excluded; Bietenholz et al. 2021). However, this luminosity limit includes rare and extremely luminous radio transients, including gamma-ray bursts and tidal disruption events (Chandra & Frail 2012; Law et al. 2018b; Ravi et al. 2022), typical AGN (Merloni et al. 2003), and hypothesized (and some recently observed) types of supernova (Chevalier 1998; Margalit & Metzger 2018; Omand et al. 2018; Dong et al. 2021).

In Table 1, we summarize the properties of FRBs with measurements or limits on PRS emission.[8] We identified 24 FRBs that are either (1) localized to arcsecond precision or (2) have limits on the distance and associated radio flux density that place an upper limit on a PRS (Connor et al. 2020b; Aggarwal et al. 2021). The radio luminosity is recalculated from the flux density/distance limit assuming cosmological parameters defined in Planck Collaboration et al. (2016). The spectral properties of PRS are not well defined, so we identify a PRS by its spectral luminosity in units of erg s^{-1} Hz^{-1} and list the radio frequency of the measurement, $\nu_{\rm PRS}$.

Four FRBs (190611, 190711, 190714, 200430) are well-localized but have no published limit on the flux density of radio counterparts. In the northern sky, the positions of FRBs 190714 and 200430 were observed by the Very Large Array (VLA) Sky Survey (Lacy et al. 2020), and in the southern sky, the positions of FRBs 190611 and 190711 were observed by the ASKAP RACS survey (McConnell et al. 2020). No counterparts were found for any of these FRBs, which sets a 3σ limit of 0.5 mJy (at 3 GHz) for 190714 and 200430 and 0.75 mJy (at 900 MHz) for 190611 and 190711. FRB 200428 (a.k.a. SGR 1935+2154) is in the Milky Way, but we consider it with an extragalactic perspective. We conservatively associate it with persistent radio emission from a ~20 pc supernova remnant (Kothes et al. 2018)[9] and treat it as a nonrepeater with no PRS, according to our definitions. Four FRBs have persistent radio emission associated with star formation: 191001 (Bhandari et al. 2020a), 190608 (Bhandari et al. 2020b), 201124A (Fong et al. 2021; Ravi et al. 2021), and 181030A (Bhardwaj et al. 2021). In these cases, the upper limit on PRS emission associated with the FRB is less than the PRS luminosity threshold, so the presence of a PRS is excluded.

For each source, we summarize the observed DM and an estimate of the DM that can be attributed to its host galaxy, including the galaxy halo, ISM, and the FRB local environment. The DM contribution can be expressed as a sum of physically distinct components:

$$\mathrm{DM} = \mathrm{DM_{MW}} + \mathrm{DM_{MW,halo}} + \mathrm{DM_{IGM}} + \mathrm{DM_{host}}/(1+z), \quad (1)$$

[6] Millisecond radio transients undergo a frequency-dependent time delay as they propagate through ionized gas. The frequency-dependent time delay is characterized by a dispersion measure (DM), which is equal to the integrated electron density n_e along the line of sight ($\mathrm{DM} \equiv \int_0^s n_e\, ds$).

[7] Here, we calculate a spectral luminosity for a flat spectral index: $L_\nu = 4\pi\, D_L^2\, S_\nu/(1+z)$, where D_L is the luminosity distance, S_ν is the flux density, and z is the redshift.

[8] During the review of this manuscript, PRS measurements were published on the arXiv, including one potential PRS counterpart to a nonrepeating FRB (Chibueze et al. 2021). We did not include those results in the current analysis, as they are still under review, but they should not significantly change the conclusions presented here.

[9] Limits on more compact radio emission are five orders of magnitude lower (Ravi et al. 2020).

Table 1
Properties of Localized FRBs with PRS Measurements

FRB	Repeats	Redshift/Distance	DM (pc cm^{-3})	DM_{host} (pc cm^{-3})	$L_{\nu,PRS}$ (erg s^{-1} Hz^{-1})	ν_{PRS}	References
121102	Yes	0.1927	558.0	185.2	2.8e29	1.6	C17 T17 L17
171020	⋯	<0.08[a]	114.0	−3.0	<1.0e28	5.5	M18 S18
180301	Yes	0.33	536.0	60.7	<1.8e29	1.5	Bh21a
180309	⋯	<0.32	263.0	−87.4	<5.9e28	3.0	A21
180916B	Yes	0.0337	349.0	74.6	<4.9e26	1.7	Mar20
180924	⋯	0.3214	361.42	−12.7	<5.7e28	6.5	B19 Bh20a
181030A	Yes	0.00385	103.5	9.4	<1.7e26[b]	3.0	Bh21b
181112	⋯	0.4755	589.27	112.5	<1.3e29	6.5	H20 Bh20a
190102	⋯	0.291	364.5	5.6	<4.2e28	6.5	H20 Bh20a
190520	Yes	0.241	1202.0	1097.4	3.0e29	3.0	N21
190523	⋯	0.66	760.8	129.1	<4.3e30	3.0	R19
190608	⋯	0.1178	339.5	171.2	<3.8e27[b]	6.5	Mac20 Bh20a
190611	⋯	0.378	321.4	−163.8	<2.9e30	0.9	H20 RACS
190614D	⋯	<1.0	959.2	−16.9	<3.0e29	1.4	L20
190711	Yes	0.522	587.4	22.4	<5.6e30	0.9	Ku21 Mac20 RACS
190714	⋯	0.2365	504.13	261.4	<7.2e29	3.0	H20 VLASS Bh19
191001	⋯	0.234	506.0	259.8	<2.1e28[b]	5.5	Bh20b
191108	⋯	<0.52	588.1	112.0	<2.6e30	1.4	C20
191228	⋯	0.243	297.5	6.2	<3.4e28	6.5	Bh21a
200120E	Yes	3.6 Mpc	87.0	−3.7	<3.1e23	1.5	Ki21
200428	⋯	12.5 kpc	332.0	−0.0	<2.0e23	1.4	Ch20 B20 K18
200430	⋯	0.16	380.1	194.0	<3.2e29	3.0	H20 VLASS Ku20
200906	⋯	0.3688	577.8	229.7	<4.3e28	6.0	Bh21a
201124A	Yes	0.098	420.0	232.6	<2.8e28	1.4	R21 F21

Notes. Upper limits are 3σ, unless otherwise noted. In some cases, no host galaxy is known, but the FRB distance is constrained. FRB names in bold have PRS detections or meaningful upper limits.
[a] We assume the published 5σ flux density limit at the max distance of $z = 0.08$ for FRB 171020. This is more conservative than presented in Mahony et al. (2018), as it allows for undetected host galaxies.
[b] PRS limit set by radio emission attributed to star formation activity in host galaxy.
References. C17 (Chatterjee et al. 2017); L17 (Law et al. 2017); R16 (Ravi et al. 2016); T17 (Tendulkar et al. 2017); M18 (Mahony et al. 2018); S18 (Shannon et al. 2018); A21 (Aggarwal et al. 2021); M20 (Marcote et al. 2020); B19 (Bannister et al. 2019); R19 (Ravi et al. 2019); M20 (Macquart et al. 2020); C20 (Connor et al. 2020b); L20 (Law et al. 2020); CH20 (CHIME/FRB Collaboration et al. 2020); B20 (Bochenek et al. 2020); Bh20a (Bhandari et al. 2020b); Bh20b (Bhandari et al. 2020a); H20 (Heintz et al. 2020); K19 (Kumar et al. 2019); K18 (Kothes et al. 2018); Ku21 (Kumar et al. 2021); Ki21 (Kirsten et al. 2021); R21 (Ravi et al. 2021); F21 (Fong et al. 2021); Bh21a (Bhandari et al. 2022); Bh21b (Bhardwaj et al. 2021); Bh19 (Bhandari et al. 2019); Ku20 (Kumar et al. 2020); RACS (McConnell et al. 2020); VLASS (Lacy et al. 2020).

with DM_{host} defined in the rest frame. The Milky Way halo DM has both theoretical and data-driven estimates that are consistent with $DM_{MW,halo} = 50\,pc\,cm^{-3}$ (Keating & Pen 2020; Platts et al. 2020; Das et al. 2021). We calculate DM_{MW} using the NE2001 Milky Way electron density model (Cordes & Lazio 2002). DM_{IGM} is calculated from a model of the average IGM (Planck Collaboration et al. 2016; Prochaska et al. 2019).

Given these classes, we show the FRB subgroups as a Venn diagram in Figure 1. Table 1 includes 24 FRBs, of which 15 have radio limits sensitive enough to detect a PRS. This subset is the basis of some subsequent analysis, so we highlight it in the figure and table with bold text. FRB 181112 is close to the limit, but formally counted as unconstrained. FRBs 171020 and 180309 are not localized, but have limits on bright radio counterparts that exclude association with a PRS. We can exclude the association of the whole sample of 24 FRBs with a PRS $L_{r,PRS} > 10^{31}$ erg s^{-1} Hz^{-1}. While a threshold of $L_{r,PRS} > 10^{28}$ erg s^{-1} Hz^{-1} would measure or constrain a PRS for five repeating FRBs and three nonrepeating FRBs. The sources identified as PRS/non-PRS do not change when scaling luminosity limits to a frequency of 3 GHz with a typical synchrotron spectral index of −0.7.

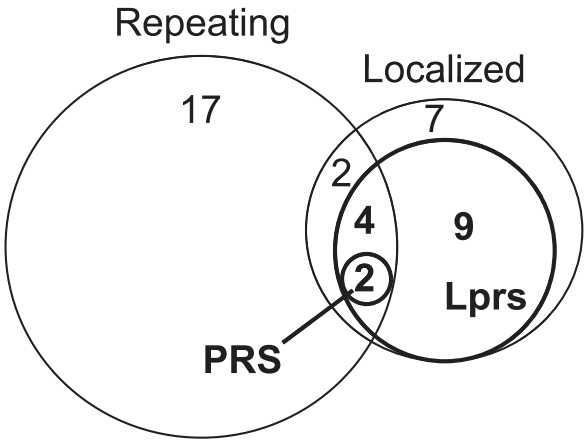

Figure 1. A Venn diagram showing how FRBs can be assigned to subgroups. The "repeating" circle includes 21 repeating FRBs listed in the Transient Name Server (http://wis-tns.org). The "localized" circle includes all sources shown in Table 1, which includes some FRBs with no host galaxy identification. The "Lprs" circle includes the subset of FRBs with detections or luminosity limits $L_{r,PRS} \leq 10^{29}$ erg s^{-1} Hz^{-1}. This sample is shown in bold here and in Table 1, and is used in subsequent analysis. Finally, the "PRS" circle shows the two localized FRBs with PRS.

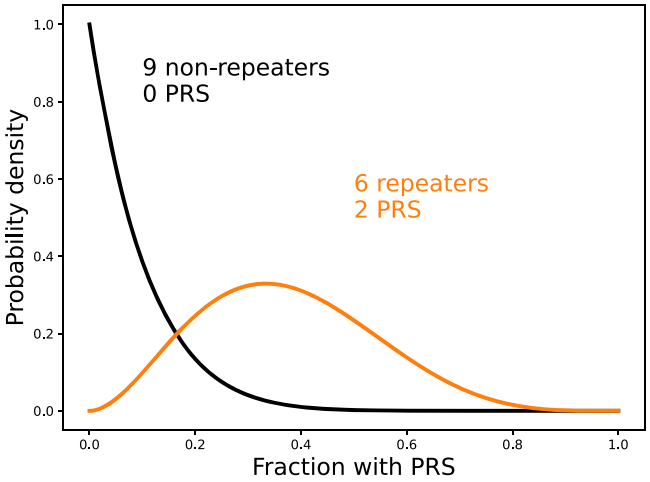

Figure 2. The PRS occurrence in repeating and nonrepeating FRBs. Fifteen FRBs (shown in bold in Table 1 and Figure 1) have deep radio imaging sensitive to PRS luminosities of 10^{29} erg s^{-1} Hz^{-1}. Curves show the binomial distribution for the repeating (orange) and nonrepeating (black) groups.

3. PRS Occurrence in FRBs

With the classification of localized FRBs into the observational categories of repeater/nonrepeater and PRS/no-PRS, we can calculate the fraction of sources in these classes. Specifically, we want to know what fraction of repeaters, $f_{\rm r}$, has a detectable persistent source relative to the fraction for nonrepeaters, $f_{\rm nr}$. Current data allow us to estimate the true $f_{\rm r}$ and $f_{\rm nr}$ values of the underlying population. We model the question with a binomial distribution. This is analogous to a biased coin flip, where one can ask: "If I flip a coin n times and it comes up heads k times, what are the allowed values for the probability of heads on this coin?" Similarly, if we observe $n_{\rm nr}$ nonrepeating FRBs and none has a PRS, we want to know the maximum allowed value of $f_{\rm nr}$. For repeating FRBs, we can calculate the allowed values of $f_{\rm r}$, given $k_{\rm r}$ out of $n_{\rm r}$ repeaters has a coincident PRS. The following two equations give the probability distributions for the PRS fraction f for repeaters and nonrepeaters:

$$p(f_{\rm r}|n_{\rm r}, k_{\rm r}) = \binom{n_{\rm r}}{k_{\rm r}} f_{\rm r}^{k_{\rm r}} (1 - f_{\rm r})^{n_{\rm r}-k_{\rm r}}, \quad (2)$$

$$p(f_{\rm nr}|n_{\rm nr}, k_{\rm nr} = 0) = \binom{n_{\rm nr}}{0} (1 - f_{\rm nr})^{n_{\rm nr}}. \quad (3)$$

Currently, there are nine localized nonrepeaters sensitive to a PRS. Given that none have been detected, we place a 90% upper limit of $f_{\rm nr} < 0.23$. There are two localized repeaters with PRS out of six searched, which gives a 90% confidence region of $0.15 < f_{\rm r} < 0.73$. The probability distributions for the two observational classes are shown in Figure 2. With current data, there is no strong evidence that PRS are preferentially found coincident with repeating FRBs. As a simple estimate, consider that the probability of two PRS showing up in a subset of six FRBs out of 15 total is given by $\frac{6}{15} \times \frac{5}{14} \approx 0.14$. If we also sum over cases as extreme or more extreme than this one (i.e., $\geqslant$2 out of 6), we find a probability closer to 0.20. But this estimate could be significantly improved with radio imaging of the eight localized FRBs that have poor constraints on $L_{\rm r,PRS}$.

We emphasize that, without further considerations, this question is strictly observational and not necessarily physical. For example, if repeating FRBs were systematically more nearby or had more sensitive images, then their PRS would be more easily detectable than nonrepeating FRBs. In the following section, we show that the PRS measurements are not strongly biased in this way.

Considering both repeating and nonrepeating FRBs, there are two of 15 with PRS counterparts, which gives a PRS fraction of $0.06 < f_{\rm all} < 0.36$ (90% confidence). This fraction is subject to an additional bias, which is the relative likelihood of localizing repeating FRBs relative to nonrepeating FRBs. Assuming that all FRBs repeat at some level, then the chance of finding an FRB is higher for FRBs that are brighter or more active. No additional bias is introduced for identifying a PRS, beyond that of FRB localization, so the PRS fraction is appropriate for the sample of detected FRBs.

4. What FRB Properties Predict the Presence of a PRS?

Here, we consider FRB properties that might explain their association with a PRS. Figure 3 shows correlations between $L_{\rm r,PRS}$, DM$_{\rm host}$, and repetition.[10] DM$_{\rm host}$ itself can be attributed to three distinct components: host galaxy halo, ISM, and the local FRB environment. The first two were considered in Macquart et al. (2020), which used localized FRBs to estimate the baryon density of the IGM. They defined a probability distribution for DM$_{\rm host}$ as

$$p_{\rm host}\,({\rm DM_{host}}|\mu,\,\sigma_{\rm host}) = \frac{1}{(2\pi)^{1/2}{\rm DM}\sigma_{\rm host}} \exp\left[-\frac{({\rm logDM} - \mu)^2}{2\sigma_{\rm host}^2}\right], \quad (4)$$

where μ and $\sigma_{\rm host}$ represent the mean and standard deviation of the host galaxy DM.

This functional form was designed to estimate the host galaxy halo and ISM contributions, not local DM. Furthermore, the FRB sample definition excluded FRB 121102 due to its anomalously large (presumably local) DM. This model finds a rest-frame halo/ISM DM contribution with mean 68 pc cm^{-3} and width parameter of 0.88, which predicts DM$_{\rm host} < 210$ (90% confidence) for the typical FRB host galaxy. This is consistent with detailed DM modeling of foreground galaxies toward FRB 180924 and 190608, which lie along relatively under- and over-dense lines of sight, respectively (Simha et al. 2020, 2021).

The bottom panel of Figure 3 shows how the measured DM$_{\rm host}$ compares to that expected from the typical FRB host. FRBs 121102 and 190520 stand out for having high PRS luminosities, large DM$_{\rm host}$, and high burst rates. In contrast, FRBs 180916B and 201124A actively repeat, but have limits on PRS emission. Clearly, repetition rate is not sufficient to predict the presence of a PRS. However, FRBs with both a large repetition rate and DM$_{\rm host}$ may be more likely to have a PRS. The large DM$_{\rm host}$ of FRB 201124A may seem to contradict this point, but we note that the host galaxy is more massive and has more star formation than the typical FRB host. To quantify this further, we collected galaxy stellar mass and star formation rate for 19 FRB host galaxies (Heintz et al. 2020;

[10] An assumption of this analysis is that the burst repetition and PRS luminosity are independent and that the PRS is not *exactly equal to* the integrated burst emission. Gourdji et al. (2019) considered whether the FRB 121102 bursts can produce its PRS. They found that 700 bursts ms^{-1} are required to produce the PRS luminosity, which is not consistent with the observed burst energy distribution.

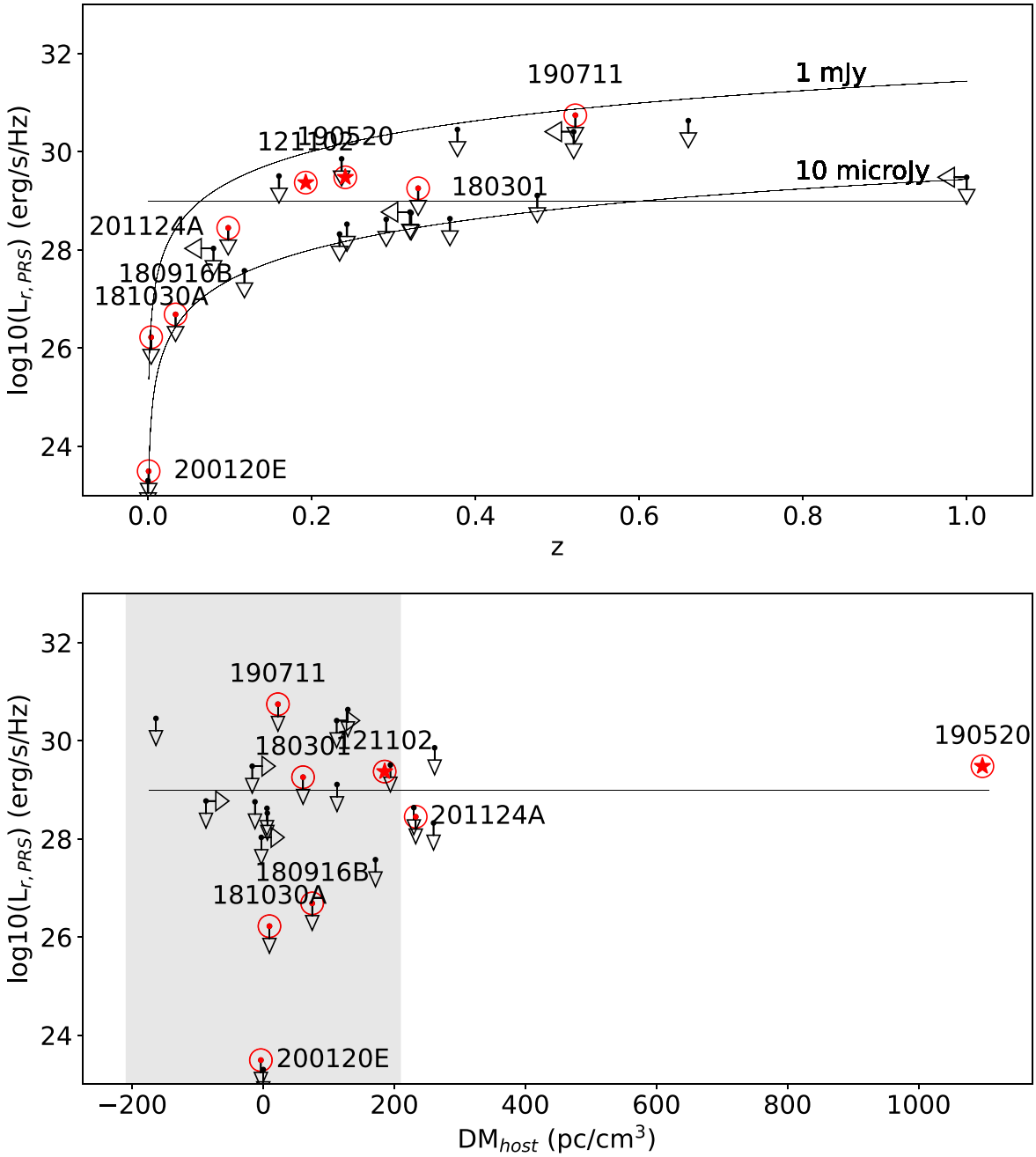

Figure 3. Top: PRS luminosity measurements or limits as a function of host galaxy redshift. Repeating FRBs are shown in red, circled, and labeled by name; PRS detections are shown as a star. The solid horizontal line shows the defined luminosity for a PRS, $L_{\rm PRS} = 10^{29}$ erg s^{-1} Hz^{-1}. The two curved lines show the luminosity limit for flux density limits of 1 mJy and 10 μJy. Bottom: PRS luminosity vs. DM$_{\rm host}$ (rest frame) for the same FRB sample. FRB 200430 (SGR 1935+2154) is assigned a DM$_{\rm host}$ of 0, which partially overlaps with FRB 200120E. The shaded region shows $|{\rm DM_{host}}| < 210$ pc cm^{-3}, which is a typical contribution of the ISM of a host galaxy.

Niu et al. 2021). Figure 4 shows that DM$_{\rm host}$ normalized by stellar mass shows that FRB 121102 and 190520 are outliers by an order of magnitude. The distinction is not as clear for DM$_{\rm host}$ normalized by SFR, with FRBs 121102, 190520, 180916, and 190523 showing relatively high values. Normalizing DM by host galaxy properties introduces significant uncertainty, since the location of the FRB in the host galaxy is not known. However, the stellar mass normalization separates the two FRBs associated with PRS, which highlights the fact that PRS are associated with relatively small galaxies.

If excess DM$_{\rm host}$ is causally connected to PRS luminosity, it would have tremendous diagnostic power. The PRS is emitted by a relativistic plasma, while the DM is caused by a physically distinct cold plasma. Some FRB source models predict local counterparts, such as H II regions, SNRs, and PWNe, that can contribute significant local DM and relativistic plasma (>100 pc cm^{-3}; Connor et al. 2016; Yang & Zhang 2017). Young magnetar and fast pulsar models have been used for detailed calculations of ionization and radiation that predict significant contribution to the FRB DM and a luminous PRS (Kashiyama & Murase 2017; Margalit & Metzger 2018). On a larger scale, calculations of SN ionized ejecta and stellar winds predict DM as high as 100–1000 pc cm^{-3} and RMs of 10^4–10^6 rad m^{-2} after 10–100 yr (Piro & Gaensler 2018). Milky Way

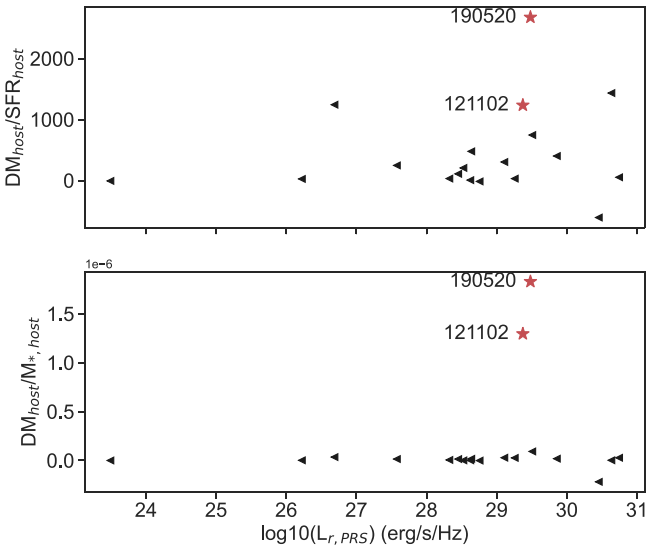

Figure 4. Top: FRB DM_{host} normalized by host galaxy star formation rate vs. PRS luminosity for 19 FRBs associated with a host galaxy. The y-axis has units of pc cm^{-3} yr $M_{\odot}^{-1}$. The two FRBs with PRS detections are shown as red stars, while all other symbols denote $L_{r,PRS}$ upper limits. Bottom: as in top panel, but DM is normalized by host galaxy stellar mass (units of pc cm^{-3} $M_{\odot}^{-1}$).

pulsars in SNRs have an excess DM (Straal et al. 2020) that is consistent with predictions of much larger excess in the younger scenarios predicted for FRBs. Alternatively, compact binary mergers have a distinctive scale for DM and RM evolution (Zhao et al. 2021).

If DM_{host} is correlated with PRS luminosity and repetition rate, then we can use this to guide follow-up observing. Table 1 and Figure 3 highlight FRB sources with large DM_{host} (>150 pc cm^3) and weak constraints on PRS emission: FRBs 190714 and 200430. Deep radio imaging and/or FRB search of these sources may be more likely to find new bursts and/or PRS emission.

In a similar vein, we have chosen a single PRS luminosity threshold of 10^{29} erg s^{-1} Hz^{-1}. This was done for the practical purpose of applying a binomial distribution based on Boolean values, while avoiding astrophysical foregrounds (see Section 2). However, physical models of PRS naturally produce a range of luminosities (e.g., based on the age of a central neutron star or accretion rate for a intermediate mass black hole). Ultimately, we will be motivated to consider a distribution of PRS luminosities and treat the problem not as binomial but continuous in the relevant observables. For example, if all FRBs are repeaters but with a wide range of activity, we ought to look for correlations between PRS luminosity and repetition rate.

Finally, we note that the top panel of Figure 3 demonstrates how PRS limits scale with distance and helps demonstrate potential bias between the repeater/nonrepeater populations. The PRS luminosity limit tends to be derived from shallow all-sky surveys or deep follow-up imaging (characteristic sensitivities are shown as lines in the figure). All-sky surveys have a completeness limit of roughly 1 mJy, which is sensitive to the PRS luminosity to a distance of $z = 0.065$ ($D_L = 300$ Mpc), while a 1 hr, 1.4 GHz VLA observation has a sensitivity of 10 μJy and is sensitive to the PRS luminosity to $z = 0.6$ ($D_L = 3.6$ Gpc). Most FRBs with meaningful PRS limits would also limit PRS emission out to $z \approx 0.4$, a distance that includes a similar number of repeating and nonrepeating FRBs. This supports the argument that PRS emission from repeaters and nonrepeaters is equally well-constrained and that the preference for PRS emission in repeating FRBs is not strongly biased by distance (Figure 2).

5. FRB Source Density

With a working definition of a PRS, we can consider how they contribute to radio source counts. First, we need to estimate the FRB source density from the volumetric rate and repetition statistics. This estimate builds on previous work (Nicholl et al. 2017; Eftekhari et al. 2020) by using data to bound the repetition rate.

The volumetric density of FRB-emitting sources can be defined as

$$\mathcal{N}_{\rm src} = \frac{\Phi_z}{\langle \mathcal{R}_{\rm src} \rangle f_{\rm b}}, \tag{5}$$

where Φ_z is the FRB volumetric rate at redshift z (in units of Gpc^{-3} yr^{-1}), $\langle \mathcal{R}_{\rm src} \rangle$ is the average burst rate per source, and $f_{\rm b}$ is the beaming fraction of FRB emission (fraction of sources with beams pointed toward us). The volumetric rate can be estimated from the detection rate of all FRBs combined with knowledge of the redshift distribution of FRBs. The estimation of this rate has been approached with a variety of techniques and data sets, and is generally consistent (Connor 2019; Lu & Piro 2019; Luo et al. 2020; Arcus et al. 2021; Gardenier et al. 2021). We use the rate of James et al. (2022), which is $\Phi_{z=0} = 9^{+2}_{-4} \times 10^4$ Gpc^{-3} yr^{-1} with burst energy greater than 10^{39} erg in the local universe.

The average burst rate per source is more difficult to entertain, because we are forced to calculate an expected value over a broad distribution of repeat rates, with significant weight at $\mathcal{R}_{\rm src} = 0$ if some FRBs are true nonrepeaters. We simplify the problem by considering the limiting cases that either (1) all FRBs repeat or that (2) there is a mix of repeaters and true nonrepeaters. We use the observed CHIME/FRB burst sample under these two cases to bound the estimated average repetition rate of FRBs. This estimate is based on the 20 publicly available CHIME/FRB repeating sources[11] and the 474 nonrepeaters in the CHIME/FRB catalog.

As a lower limit on $\langle \mathcal{R}_{\rm src} \rangle$, assume that all sources only detected once at CHIME/FRB are true nonrepeaters with rate zero. Then assume there are no values of $\mathcal{R}_{\rm src}$ higher than the most active CHIME repeater. By a simple weighted average, this gives

$$\langle \mathcal{R}_{\rm src} \rangle_{\rm low} = \frac{1}{N_{\rm R} + N_{\rm NR}} (N_{\rm R} \langle \mathcal{R}_{\rm R} \rangle + N_{\rm NR} \langle \mathcal{R}_{\rm NR} \rangle), \tag{6}$$

where $N_{\rm R}$ and $N_{\rm NR}$ are the numbers of repeaters and nonrepeaters in the CHIME/FRB sample. The available CHIME/FRB repeaters have a mean repeat rate of roughly 580 bursts per year, assuming each has been observed since 2018 August for 10 minutes per source per day. Using 474 nonrepeaters and 20 repeaters, we find $\langle \mathcal{R}_{\rm src} \rangle_{\rm low} \approx 25$ yr^{-1}.

The upper limit on the average rate (and lower bound on the density of sources) comes from assuming that all FRBs detected by CHIME/FRB are repeaters, but the survey has not been on sky long enough to detect some of them more than

[11] https://www.chime-frb.ca/repeaters

once. We assume that all FRBs obey a power-law distribution in repetition rate with a probability density function, $n(\mathcal{R}) \propto \mathcal{R}^{-\alpha}$. We determine α empirically from the CHIME/FRB repeaters to be $\approx$1.5, using the maximum-likelihood estimator from Crawford et al. (1970). The expected value in this case is

$$\langle \mathcal{R}_{\rm src} \rangle_{\rm up} = \int_{\mathcal{R}_{\rm min}}^{\mathcal{R}_{\rm max}} \mathcal{R}\, n(\mathcal{R})\, d\mathcal{R}. \quad (7)$$

Replacing $n(\mathcal{R})$ with an integration constant times the power law, $C\,\mathcal{R}^{-\alpha}$, we get

$$\langle \mathcal{R}_{\rm src} \rangle_{\rm up} = \frac{C}{2-\alpha}(\mathcal{R}_{\rm max}^{2-\alpha} - \mathcal{R}_{\rm min}^{2-\alpha}). \quad (8)$$

We take $\mathcal{R}_{\rm max}$ to be the highest rate of any CHIME FRB, and $\mathcal{R}_{\rm min}$ to be the reciprocal of the total exposure per source since CHIME/FRB first light, $1/T_{\rm tot}$. To reiterate, in this scenario we are assuming that all CHIME sources are repeaters, and the FRBs that have only been detected once simply have low activity with $\mathcal{R} \lesssim 2/T_{\rm tot}$. Plugging these values into Equation (8) gives $\langle \mathcal{R}_{\rm src} \rangle_{\rm up} = 440\ {\rm yr}^{-1}$.

Given the bounds on repetition and the volumetric FRB rate, we can calculate the density of FRB-emitting sources. Using the 2σ range on the volumetric rate, we bound the source density, $2.2 \times 10^2 f_{\rm b,0.1}^{-1}\,{\rm Gpc}^{-3} < \mathcal{N}_{\rm src} < 5.2 \times 10^4 f_{\rm b,0.1}^{-1}\,{\rm Gpc}^{-3}$, where $f_{\rm b,0.1} = f_{\rm b}/0.1$ is a parameterized beaming fraction. The value of $f_{\rm b}$ can vary widely with emission mechanism, with a characteristic value of 1/10 for pulsars (Tauris & Manchester 1998; O'Shaughnessy & Kim 2010) and potentially much smaller values for coherent emission mechanisms (Cordes & Wasserman 2016; Katz 2017a).

This constraint is built on assumptions of burst energy and repetition. This FRB volumetric rate is based on an energy limit ($E > 10^{39}$ erg) that corresponds to a burst fluence of 15 Jy ms in 256 MHz at $z = 0.1$. This distance is roughly equal to that which defines a complete volume for the sample of precommissioning FRBs seen by CHIME/FRB, as discussed in Ravi (2019). With a lower flux density threshold, a more powerful survey could go further down the FRB luminosity function and perhaps have access to more sources in a given volume. The repetition statistics are derived from CHIME/FRB sources, which may differ from those seen by other telescopes (e.g., based on pulse width, DM/scattering distribution, emission frequency).

6. PRS in the Wild

PRS are as luminous as AGN, the most common class of extragalactic radio source (Condon et al. 2019). Given that AGN are detectable at great distances, it is reasonable to wonder whether FRB sources may be detectable via their PRS counterparts. Here, we use the bound on FRB source density from Section 5 to estimate the density of PRS, their contribution to radio source catalogs, and prospects for identifying them independent of their FRB emission.

For an FRB source density of $\mathcal{N}_{\rm src}$, we expect a PRS density of $\mathcal{N}_{\rm PRS} = f_{\rm all}\,\mathcal{N}_{\rm src}$. In Section 3, we estimated the PRS occurrence to be between 0.06 and 0.36, which we parameterize to a value of $f_{\rm all} = 0.2$. Thus, we find $\mathcal{N}_{\rm PRS} \approx 50$–$10000\, f_{\rm b,0.1}^{-1}\, f_{\rm all,0.2}\,{\rm Gpc}^{-3}$. Table 2 summarizes the bounds on FRB and PRS densities and rates.

At this density, radio source catalogs and new sky surveys should detect a significant number of PRS. The FIRST, VLASS, and RACS radio surveys are complete to a flux density of roughly 1 mJy, which detects all PRS out to a distance of $z = 0.065$ (luminosity distance of 300 Mpc). For an all-sky survey (typically seeing 3π steradians), these surveys are sensitive to these sources in a volume of 0.08 Gpc^3, which includes 4–830 $f_{\rm b,0.1}^{-1}\, f_{\rm all,0.2}$ PRS. This likely underestimates the number of detectable sources, because it assumes a fixed PRS luminosity of $10^{29}\,{\rm erg\,s^{-1}\,Hz^{-1}}$. The two known PRS have luminosities three times larger than that and would be detectable over a larger volume.

Table 2
FRB and PRS Rates and Densities

Parameter	Symbol	Range (90% CI)
Repetition rate	$\langle \mathcal{R}_{\rm src} \rangle$	25–440 yr^{-1}
FRB source density	$\mathcal{N}_{\rm src}$	220–52,000 $f_{\rm b,0.1}^{-1}$ Gpc^{-3}
PRS fraction	$f_{\rm all}$	0.06–0.36
PRS density	$\mathcal{N}_{\rm PRS}$	50–10,000 $f_{\rm b,0.1}^{-1}\, f_{\rm all,0.2}$ Gpc^{-3}

Note. Estimate is appropriate for sources that emit FRBs with an energy $> 10^{39}$ erg at $z = 0$, as calculated in James et al. (2022).

By number, PRS are a small fraction (10^{-5}–10^{-3}) of a typical radio catalog (e.g., VLASS epoch 1 catalog has 1.7×10^6 sources; Gordon et al. 2021). Condon et al. (2019) use radio and infrared emission to classify extragalactic radio sources in the local universe. For luminosities greater than $10^{29}\,{\rm erg\,s^{-1}\,Hz^{-1}}$ the respective densities of star-forming galaxies and AGN are 1.4×10^5 and $1.0 \times 10^6\,{\rm Gpc}^{-3}$. So in the local universe, PRS potentially amount to as much 1% and 7% of the radio-luminous AGN and star-forming galaxy populations, respectively.

7. Discussion and Conclusions

A remarkable fact about FRBs is that their volumetric rate is roughly equal to that of core-collapse supernovae, $\Phi_{\rm ccsn} = 10^{+5}_{-3.5} \times 10^4\,{\rm Gpc}^{-3}\,{\rm yr}^{-1}$ (Cappellaro et al. 2015; Perley et al. 2020, at $z = 0$). The rate scales with energy as $R(>E_\nu) \propto E_\nu^{-1}$, so low-energy FRBs are more abundant (Lu et al. 2022). Plausible progenitor channels are too rare to explain the FRB volumetric rate (Ravi 2019), and sources at low energy must either be emitted by more abundant sources or have a higher repetition rate (Bhardwaj et al. 2021).

The most detailed physical models for repeating FRBs are based upon magnetars (Kashiyama & Murase 2017; Margalit & Metzger 2018). The magnetars that produce flaring events as soft-gamma repeaters (SGR) have been characterized well. SGR flares occur at a rate of $3.8^{+4.0}_{-3.1} \times 10^5\,{\rm Gpc}^{-3}\,{\rm yr}^{-1}$ above an energy of 4×10^{44} erg (Burns et al. 2021), which is comparable to the FRB rate above 10^{39} erg (James et al. 2022). The ratio of energy in these two bands, referred to as η, is 4×10^5, which is consistent with some theoretical models and observational constraints (Chen et al. 2020; Tavani et al. 2021).

In estimating the mean FRB repetition rate, we have considered two scenarios: (1) all FRBs repeat with a rate drawn from a power-law distribution and (2) some FRBs repeat and some are cataclysmic. Analysis of FRB spectra and temporal widths have also been used to argue that repeating and nonrepeating FRBs are distinct classes (CHIME/FRB Collaboration et al. 2019; Fonseca et al. 2020; Pleunis & Chime/Frb Collaboration 2021). Here, we identify PRS emission as a potential new signature of a distinct subpopulation of FRBs. If true, PRS is likely to be more useful in defining classes, since it can more easily be connected to simple

physical parameters (e.g., energy input, age; Kashiyama & Murase 2017; Metzger et al. 2017).

As more sources are localized and more FRB local environments are studied, other relationships may become apparent (e.g., Faraday rotation measure, scattering, stellar environment). The stellar environment of the FRB is also easier to interpret physically (e.g., mean age of progenitors; Mannings et al. 2021). Generally, the distribution of FRB host galaxy properties suggest that FRBs trace the cosmic star formation rate (Bochenek et al. 2021). However, if FRBs with PRS tend to form in small, star-forming galaxies, it may favor the idea that they are formed by a process that differs from that of nonrepeating FRBs.

In this work, we bound the FRB source density in order to compare it to other classes of object. Table 2 summarizes bounds on rates and densities for both FRB sources and PRS. The FRB source density estimate is consistent with that of Lu & Kumar (2016), which assumed that all FRB sources are emitted by neutron stars and repeat with some universal energy distribution.

The consistency of burst rates with predictions from magnetar models belies the fact that magnetars are far more common than FRB sources. Magnetars constitute a significant fraction ($\sim$0.4) of the neutron star population and are born at a rate of roughly $10^{-2}\,\mathrm{yr}^{-1}$ in the Milky Way (Beniamini et al. 2019). Given that most of their energy is stored in the magnetic field that decays on a timescale of 10^4 yr, roughly 100 magnetars are present in a Milky Way–like galaxy at any time. The density of Milky Way–like galaxies is $\Phi_{\mathrm{MW}} \approx 10^7\,\mathrm{Gpc}^{-3}$ (Blanton et al. 2003), so the density of magnetars is roughly $10^9\,\mathrm{Gpc}^{-3}$. This is a factor of 10^6 larger than the FRB source density (consistent with independent estimates; Lu et al. 2022). If magnetars do emit FRBs, then they must occur in a tiny subset of all magnetars, such as the youngest or most magnetic sources.

We have also used the prevalence of PRS in FRBs to estimate their contribution to the persistent radio source population. By definition, PRS are associated with FRBs, so this provides a complementary way to test models for FRB origin. Interestingly, PRS look remarkably similar to compact, low-luminosity AGN. As discussed above, the volumetric density of galaxies (and their supermassive black holes) is many orders of magnitude larger than the PRS density, but subclasses do occur at a comparable level (e.g., AGN identified via their broad-line emission; Greene & Ho 2007).

PRS are distinctive for being compact, radio luminous, and associated with star formation (Mannings et al. 2021; Tendulkar et al. 2021). However, it is important to note that the nonnuclear location of the two known PRS does not preclude their association with AGN. Reines et al. (2020) identified dozens of luminous (some nonnuclear) radio sources in dwarf galaxies that are consistent with AGN, so-called "wandering black holes." This search was complete to VLA/FIRST radio sources in dwarf galaxies within 225 Mpc and identified five with luminosities consistent with a PRS. Given the footprint of the surveys, we estimate a volumetric density of $4 \times 10^2\,\mathrm{Gpc}^{-3}$. Therefore, the density of PRS is consistent with that of candidate AGN in dwarf galaxies. This is consistent with a relative rate density estimated in Eftekhari et al. (2020), which also details the phenomenological similarity of the PRS with AGN in the sample of Reines et al. (2020).

An FRB maximalist may be tempted to categorize "wandering black holes" as PRS. However, there is significant theoretical and observational motivation for the existence of off-nuclear AGN (Greene et al. 2020; Ward et al. 2021). In many cases, the luminous radio emission can be directly attributed to accretion onto a black hole (Mezcua & Domínguez Sánchez 2020; Molina et al. 2021). Given the uncertain nature of PRS, it is also possible that off-nuclear AGN produce PRS and FRBs (Katz 2017b; Zhang 2020)!

The ambiguity between AGN and PRS argues for caution when classifying based on radio data alone. Nuclear radio sources are likely to be AGN and off-nuclear radio sources may be a PRS, but gas dynamics and ionization are required to show that definitively. Given the similar densities of PRS and AGN in dwarf galaxies, it is likely that PRS have already been detected and perhaps misidentified as AGN (Mezcua et al. 2019).

We acknowledge helpful discussions with Wenbin Lu, Kazumi Kashiyama, and Vikram Ravi. C.J.L. acknowledges support from the National Science Foundation under grant No. 2022546. K.A. acknowledges support from NSF grants AAG-1714897 and #2108673.

Facility: EVLA, ASKAP.

Software: astropy (Astropy Collaboration et al. 2018).

ORCID iDs

Casey J. Law https://orcid.org/0000-0002-4119-9963
Liam Connor https://orcid.org/0000-0002-7587-6352
Kshitij Aggarwal https://orcid.org/0000-0002-2059-0525

References

Aggarwal, K., Burke-Spolaor, S., Tejos, N., et al. 2021, ApJ, 913, 78
Arcus, W. R., Macquart, J. P., Sammons, M. W., James, C. W., & Ekers, R. D. 2021, MNRAS, 501, 5319
Astropy Collaboration, Price-Whelan, A. M., Sipőcz, B. M., et al. 2018, AJ, 156, 123
Bannister, K. W., Deller, A. T., Phillips, C., et al. 2019, Sci, 365, 565
Beniamini, P., Hotokezaka, K., van der Horst, A., & Kouveliotou, C. 2019, MNRAS, 487, 1426
Bhandari, S., Bannister, K. W., Lenc, E., et al. 2020a, ApJL, 901, L20
Bhandari, S., Heintz, K. E., Aggarwal, K., et al. 2022, AJ, 163, 69
Bhandari, S., Kumar, P., Shannon, R. M., & Macquart, J. P. 2019, ATel, 12940, 1
Bhandari, S., Sadler, E. M., Prochaska, J. X., et al. 2020b, ApJL, 895, L37
Bhardwaj, M., Kirichenko, A. Y., Michilli, D., et al. 2021, ApJL, 919, L24
Bietenholz, M. F., Bartel, N., Argo, M., et al. 2021, ApJ, 908, 75
Blanton, M. R., Hogg, D. W., Bahcall, N. A., et al. 2003, ApJ, 592, 819
Bochenek, C. D., Ravi, V., Belov, K. V., et al. 2020, Natur, 587, 59
Bochenek, C. D., Ravi, V., & Dong, D. 2021, ApJL, 907, L31
Burns, E., Svinkin, D., Hurley, K., et al. 2021, ApJL, 907, L28
Cappellaro, E., Botticella, M. T., Pignata, G., et al. 2015, A&A, 584, A62
Chandra, P., & Frail, D. A. 2012, ApJ, 746, 156
Chatterjee, S., Law, C. J., Wharton, R. S., et al. 2017, Natur, 541, 58
Chen, G., Ravi, V., & Lu, W. 2020, ApJ, 897, 146
Chevalier, R. A. 1998, ApJ, 499, 810
Chibueze, J. O., Caleb, M., Spitler, L., et al. 2021, arXiv:2201.00069
Chime/Frb Collaboration, Amiri, M., Andersen, B. C., et al. 2020, Natur, 582, 351
CHIME/FRB Collaboration, Andersen, B. C., Bandura, K., et al. 2019, ApJL, 885, L24
CHIME/FRB Collaboration, Andersen, B. C., Bandura, K. M., et al. 2020, Natur, 587, 54
Condon, J. J., Matthews, A. M., & Broderick, J. J. 2019, ApJ, 872, 148
Connor, L. 2019, MNRAS, 487, 5753
Connor, L., Miller, M. C., & Gardenier, D. W. 2020a, MNRAS, 497, 3076
Connor, L., Sievers, J., & Pen, U.-L. 2016, MNRAS, 458, L19
Connor, L., van Leeuwen, J., Oostrum, L. C., et al. 2020b, MNRAS, 499, 4716
Cordes, J. M., Bhat, N. D. R., Hankins, T. H., McLaughlin, M. A., & Kern, J. 2004, ApJ, 612, 375
Cordes, J. M., & Chatterjee, S. 2019, ARA&A, 57, 417

Cordes, J. M., & Lazio, T. J. W. 2002, arXiv:astro-ph/0207156
Cordes, J. M., & Wasserman, I. 2016, MNRAS, 457, 232
Crawford, D. F., Jauncey, D. L., & Murdoch, H. S. 1970, ApJ, 162, 405
Das, S., Mathur, S., Gupta, A., Nicastro, F., & Krongold, Y. 2021, MNRAS, 500, 655
Dong, D. Z., Hallinan, G., Nakar, E., et al. 2021, Sci, 373, 1125
Eftekhari, T., Berger, E., Margalit, B., Metzger, B. D., & Williams, P. K. G. 2020, ApJ, 895, 98
Fong, W.-f., Dong, Y., Leja, J., et al. 2021, ApJL, 919, L23
Fonseca, E., Andersen, B. C., Bhardwaj, M., et al. 2020, ApJL, 891, L6
Gardenier, D. W., Connor, L., van Leeuwen, J., Oostrum, L. C., & Petroff, E. 2021, A&A, 647, A30
Gordon, Y. A., Boyce, M. M., O'Dea, C. P., et al. 2021, ApJS, 255, 30
Gourdji, K., Michilli, D., Spitler, L. G., et al. 2019, ApJL, 877, L19
Greene, J. E., & Ho, L. C. 2007, ApJ, 667, 131
Greene, J. E., Strader, J., & Ho, L. C. 2020, ARA&A, 58, 257
Heintz, K. E., Prochaska, J. X., Simha, S., et al. 2020, ApJ, 903, 152
Hilmarsson, G. H., Michilli, D., Spitler, L. G., et al. 2021, ApJL, 908, L10
James, C. W., Prochaska, J. X., Macquart, J. P., et al. 2022, MNRAS, 510, L18
Kashiyama, K., & Murase, K. 2017, ApJL, 839, L3
Katz, J. I. 2017a, MNRAS, 467, L96
Katz, J. I. 2017b, MNRAS, 471, L92
Katz, J. I. 2021, MNRAS, 501, L76
Keating, L. C., & Pen, U.-L. 2020, MNRAS, 496, L106
Kirsten, F., Marcote, B., Nimmo, K., et al. 2021, arXiv:2105.11445
Kocz, J., Ravi, V., Catha, M., et al. 2019, MNRAS, 489, 919
Kothes, R., Sun, X., Gaensler, B., & Reich, W. 2018, ApJ, 852, 54
Kumar, P., Day, C. K., Shannon, R. M., et al. 2020, ATel, 13694, 1
Kumar, P., Shannon, R. M., Flynn, C., et al. 2021, MNRAS, 500, 2525
Kumar, P., Shannon, R. M., Osłowski, S., et al. 2019, ApJL, 887, L30
Lacy, M., Baum, S. A., Chandler, C. J., et al. 2020, PASP, 132, 035001
Law, C., Tendulkar, S., Clarke, T., Aggarwal, K., & Bethapudy, S. 2021, ATel, 14526, 1
Law, C. J., Abruzzo, M. W., Bassa, C. G., et al. 2017, ApJ, 850, 76
Law, C. J., Bower, G. C., Burke-Spolaor, S., et al. 2018a, ApJS, 236, 8
Law, C. J., Butler, B. J., Prochaska, J. X., et al. 2020, ApJ, 899, 161
Law, C. J., Gaensler, B. M., Metzger, B. D., Ofek, E. O., & Sironi, L. 2018b, ApJL, 866, L22
Lorimer, D. R., Bailes, M., McLaughlin, M. A., Narkevic, D. J., & Crawford, F. 2007, Sci, 318, 777
Lu, W., Beniamini, P., & Kumar, P. 2022, MNRAS, 510, 1867
Lu, W., & Kumar, P. 2016, MNRAS, 461, L122
Lu, W., & Piro, A. L. 2019, ApJ, 883, 40
Luo, R., Lee, K., Lorimer, D. R., & Zhang, B. 2018, MNRAS, 481, 2320
Luo, R., Men, Y., Lee, K., et al. 2020, MNRAS, 494, 665
Lyu, F., Meng, Y.-Z., Tang, Z.-F., et al. 2021, FrPhy, 16, 24503
Macquart, J.-P., Bailes, M., Bhat, N. D. R., et al. 2010, PASA, 27, 272
Macquart, J. P., Prochaska, J. X., McQuinn, M., et al. 2020, Natur, 581, 391
Mahony, E. K., Ekers, R. D., Macquart, J.-P., et al. 2018, ApJL, 867, L10
Mannings, A. G., Fong, W.-f., Simha, S., et al. 2021, ApJ, 917, 75
Marcote, B., Nimmo, K., Hessels, J. W. T., et al. 2020, Natur, 577, 190
Margalit, B., & Metzger, B. D. 2018, ApJL, 868, L4
McConnell, D., Hale, C. L., Lenc, E., et al. 2020, PASA, 37, e048
Merloni, A., Heinz, S., & di Matteo, T. 2003, MNRAS, 345, 1057
Metzger, B. D., Berger, E., & Margalit, B. 2017, ApJ, 841, 14
Mezcua, M., & Domínguez Sánchez, H. 2020, ApJL, 898, L30
Mezcua, M., Suh, H., & Civano, F. 2019, MNRAS, 488, 685
Michilli, D., Seymour, A., Hessels, J. W. T., et al. 2018, Natur, 553, 182
Molina, M., Reines, A. E., Greene, J. E., Darling, J., & Condon, J. J. 2021, ApJ, 910, 5
Murase, K., Kashiyama, K., & Mészáros, P. 2016, MNRAS, 461, 1498
Nicholl, M., Williams, P. K. G., Berger, E., et al. 2017, ApJ, 843, 84
Niu, C. H., Aggarwal, K., Li, D., et al. 2021, arXiv:2110.07418
Omand, C. M. B., Kashiyama, K., & Murase, K. 2018, MNRAS, 474, 573
Oostrum, L. C., Maan, Y., van Leeuwen, J., et al. 2020, A&A, 635, A61
O'Shaughnessy, R., & Kim, C. 2010, ApJ, 715, 230
Parra, R., Conway, J. E., Diamond, P. J., et al. 2007, ApJ, 659, 314
Perley, D. A., Fremling, C., Sollerman, J., et al. 2020, ApJ, 904, 35
Petroff, E., Hessels, J. W. T., & Lorimer, D. R. 2019, A&ARv, 27, 4
Piro, A. L., & Gaensler, B. M. 2018, ApJ, 861, 150
Planck Collaboration, Ade, P. A. R., Aghanim, N., et al. 2016, A&A, 594, A13
Platts, E., Prochaska, J. X., & Law, C. J. 2020, ApJL, 895, L49
Pleunis, Z., Good, D. C., Kaspi, V. M., et al. 2021, ApJ, 923, 1
Pleunis, Z. & Chime/Frb Collaboration 2021, AAS Meeting Abstracts, 53, 236.03
Prochaska, J. X., Simha, S., Law, C., Tejos, N. M. & mneeleman 2019, FRBs/FRB: First DOI Release of this Repository, v1.0.0, Zenodo, doi:10.5281/zenodo.3403651
Rajwade, K., Stappers, B., Williams, C., et al. 2021, arXiv:2103.08410
Rajwade, K. M., Mickaliger, M. B., Stappers, B. W., et al. 2020, MNRAS, 495, 3551
Ravi, V. 2019, NatAs, 3, 928
Ravi, V., Catha, M., D'Addario, L., et al. 2019, Natur, 572, 352
Ravi, V., Dykaar, H., Codd, J., et al. 2022, ApJ, 925, 220
Ravi, V., Hallinan, G., & Law, C. J. 2020, ATel, 13693, 1
Ravi, V., Law, C. J., Li, D., et al. 2021, arXiv:2106.09710
Ravi, V., Shannon, R. M., Bailes, M., et al. 2016, Sci, 354, 1249
Reines, A. E., Condon, J. J., Darling, J., & Greene, J. E. 2020, ApJ, 888, 36
Shannon, R. M., Macquart, J. P., Bannister, K. W., et al. 2018, Natur, 562, 386
Simha, S., Burchett, J. N., Prochaska, J. X., et al. 2020, ApJ, 901, 134
Simha, S., Tejos, N., Prochaska, J. X., et al. 2021, ApJ, 921, 134
Straal, S. M., Connor, L., & van Leeuwen, J. 2020, A&A, 634, A105
Tauris, T. M., & Manchester, R. N. 1998, MNRAS, 298, 625
Tavani, M., Casentini, C., Ursi, A., et al. 2021, NatAs, 5, 401
Tendulkar, S. P., Bassa, C. G., Cordes, J. M., et al. 2017, ApJL, 834, L7
Tendulkar, S. P., Gil de Paz, A., Kirichenko, A. Y., et al. 2021, ApJL, 908, L12
The CHIME/FRB Collaboration, Amiri, M., et al. 2021, ApJS, 257, 59
Ward, C., Gezari, S., Frederick, S., et al. 2021, ApJ, 913, 102
Yang, Y.-P., & Zhang, B. 2017, ApJ, 847, 22
Zhang, B. 2020, Natur, 587, 45
Zhao, Z. Y., Zhang, G. Q., Wang, Y. Y., Tu, Z.-L., & Wang, F. Y. 2021, ApJ, 907, 111